Crystallization Behavior of Hydrogenated Sunflowerseed Oil: Kinetics and Polymorphism

M.L. Herrera
Centro de Investigación y Desarrollo en Criotecnología de Alimentos, 1900 La Plata, Argentina

Kinetics of crystallization of hydrogenated sunflowerseed oil was studied by means of an optical method. Two different aspects were examined: the effects of preheating of the molten liquid on induction time of isothermal crystallization and the effects of cooling rate on the crystallization behavior. Induction time for crystallization was markedly dependent on the crystallization temperature and the cooling rate selected. Morphology, polymorphism and chemical composition of the crystals were examined. At all crystallization temperatures, β′-form was found for the first occurring crystals. Long spacings were also similar in all cases and corresponded to a double chainlength arrangement. The chemical composition of the crystals showed no differences at either cooling rate. However, the melting behavior was different. At a slow cooling rate, fractionation occurred, and differential scanning calorimetry diagrams had a broad second endotherm with three peaks, none of which were completely resolved. The polymorphic transformation rate from β′ to β was slower when induction times were longer.

KEY WORDS: Chemical composition, crystallization, kinetics, morphology, polymorphic transformation rate, polymorphism, thermal behavior.

Sunflowerseed oil is consumed as salad or cooking oil and is modified by hydrogenation to formulate edible solid fats, such as margarines and shortenings. Formulation has a marked effect on the crystalline form attained by the end products. The desired physical properties dictate the required crystallization form and habit. For example, β′ crystals are required for margarines because they contribute to the creaming ability. β Crystals are desirable because their physical dimensions prevent the crystals from settling. Hydrogenated sunflowerseed oil has been reported as having a β tendency (1), according to the crystalline structure to which it leads. Therefore, crystallization behavior is fundamental to elucidate physical and chemical properties. The habits of hydrogenated sunflowerseed and its blends with hydrogenated cottonseed oil have been studied to obtain information to formulate and to determine suitable processing conditions for margarines and shortenings (2).

During the hydrogenation process, the double bonds within the fatty acids travel across the fatty acid chains, resulting in positional and *trans* isomers (3–6). Formation of *trans* isomers influences the chemical and physical characteristics of the final product because *trans* isomers have higher melting points and greater stability than *cis* fatty acids (7). In addition, *trans* and *cis* isomers have different polymorphic behaviors. It is well known that tripalmitoylglycerol and tristearoylglycerol are β-tending triacylglycerols. The *trans* fatty acids behave like stearic acid. In vegetable oils, 16:0 is mainly located in the *sn*-1 or *sn*-3 position of the glycerol group. So, fraction C50 consists mainly of PEP or PSP, and C52 of PEE or PSS (P, palmitic acid; S, stearic acid; E, elaidic acid). These triacylglycerols are more stable in the β form (8). deMan *et al.* (9) examined the occurrence of the β′ form in a series of vegetable fats and oils while taking into account their chemical compositions.

It should be apparent from the relatively complex polymorphism of triacylglycerols, especially those with mixed chains, that mixtures of triacylglycerols may demonstrate even more complex behavior (10). Perron *et al.* (11) established the importance of the relationship between polymorphism and intersolubility in triacylglycerol crystallization phenomenon. Gibon *et al.* (12) were the first to study phase diagrams that included stable and unstable forms of the oleic (O), (P) and (S) triacylglycerols PPP, PSP and POP. The E triacylglycerols (EEE, PEP, EPP and PEE) were also studied (13).

Crystallization behavior and thermal properties of hydrogenated sunflowerseed oil have been related to its chemical composition (14,15). When the hydrogenated oil is crystallized from the melted state, the β′ polymorphic form was observed at a wide range of cooling rates. Intersolubility of triacylglycerols has been shown to be important in the understanding of their thermal behavior (16).

The aim of the present work is to study the kinetics of isothermal crystallization of hydrogenated sunflowerseed oil by means of an optical method to carefully analyze the crystallization behavior as examined under varying temperature conditions. Morphological properties of the first-occurring crystals were examined, and their chemical composition was determined. So, additional information about the relationship between crystallization behavior and chemical composition was obtained.

MATERIALS AND METHODS

Starting oil. The oil was supplied by Molinos Rio de La Plata S.A. (Buenos Aires, Argentina). It consisted of refined hydrogenated sunflowerseed oil, with a Mettler dropping (MDP) point of 35. It was filtered in liquid state at *ca.* 80°C to eliminate dust through a 53 GA Pyrex filter.

Isothermal crystallization. The crystallization process was monitored by using the optical set-up shown in Figure 1. This equipment is an improvement of that used by Chong and Sato (17) and was described at the 1994 American Oil Chemists' Society Annual Meeting & Expo in Atlanta, Georgia (18). A helium–neon laser was used as the light source. The sample, *ca.* 20 g, was contained in a water-jacketed glass cell. A polarizer was put between the laser and the cell. The temperature of the glass cell was controlled by means of water that was circulated from two water baths attached *via* ball valves. The temperature of one bath was set at the preheating temperature (T_h), and the other was set at the crystallization temperature (T_c). The light transmitted by the crystals was then passed through the second analyzer placed at the Cross-Nicols position with the first analyzer. This enables the photodiode to detect the occurrence of optically anisotropic fat crystals. The photosensor output was recorded on a chart-recorder (model 4110, Yokogawa, Tokyo, Japan), together with the cell temperature (copper–constantin thermocouple). The sensitivity of the photodiode was

*Address correspondence at CIDCA, Casilla de Correo 553, (1900) La Plata, Argentina.

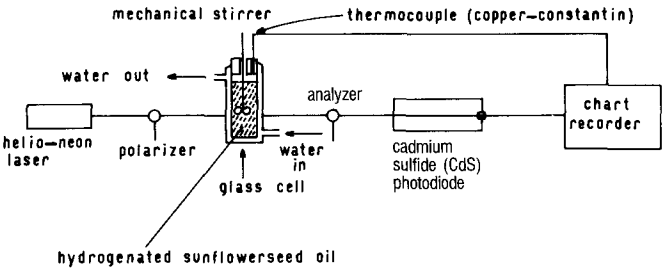

FIG. 1. Optical system for the study of induction time for the onset of crystallization of hydrogenated sunflowerseed oil.

checked with glutamic acid, which crystallized from a saturated aqueous solution. A crystal concentration of 10 ppm could be detected.

Figure 2 shows a typical chart-recorder output of the CdS photodiode, as well as the thermocouple's record for the crystallization of hydrogenated sunflowerseed oil. The induction time is the interval between the moment T_c is reached and the start of crystallization (first deviation from the laser baseline signal) (19). It was calculated as indicated in the figure.

Cooling rates were calculated from the slopes of the cell temperature record. When samples were crystallized by cooling down from $T_h = 80°C$, rates were faster than from $T_h = 40°C$ for all T_c.

Thermal treatments. The hydrogenated sunflowerseed oil in the glass cell, mechanically stirred by a motorized stirrer at a fixed speed (120 rpm), was subjected to one of two preheating treatments: (i) kept at 80°C for 30 min; or (ii) kept at 65°C for 1 h and then at 40°C for 30 min.

After the preheating period, the glass cell temperature was rapidly lowered by switching the glass cell water jacket to the water bath set at the crystallization temperature, and the first crystal occurrence was monitored. T_c of 30.7, 28.7, 27.7, 26.7 and 25.4°C were selected. Each of the two thermal treatments was carried out over five runs, and induction times presented are the average.

At the completion of a run, the sample was filtered under vacuum with a 53 GA Pyrex filter (pore diameter 5 μm). The solids were then analyzed for their polymorphic form by X-ray diffractometry and differential scanning calorimetry, and for their chemical composition by high-performance liquid chromatography (HPLC) and capillary gas chromatography (GC).

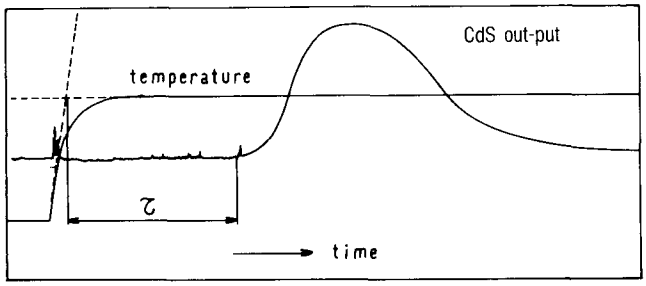

FIG. 2. Typical CdS photodiode chart-recorder output of polarization method corresponding to kinetic crystallization of hydrogenated sunflowerseed oil.

Optical microscope. The first-occurring crystals, which are defined as the crystals present in the cell when the laser signal reaches the maximum, were observed under an optical microscope Olympus CK 2 (Olympus, Tokyo, Japan). Magnification of 100 × was used for all photographs. Crystals were caught with a pipette from the growth cell and photographed in a glass cell kept at crystallization temperature.

XRD. Short spacings were measured by means of XRD (Rigaku, Tokyo, Japan) (Cu K_α $\lambda = 0.1542$ nm) at room temperature. The polymorphic transformation was induced by tempering the sample at 25°C, which was placed on the glass plate used for XRD. Small-angle XRD (rotarflex, Cu K_α, 60 Kv, 200 mA, 2θ scan from 0.1 to 5.0; Rigaku) was used to measure long spacings. XRD patterns were taken at 20, 25, 30, 35 and 40°C.

Differential scanning calorimetry (DSC). Thermal behavior was studied with a DSC 50 AC 100 (Shimadzu, Kyoto, Japan); heating rate was 5°C/min from 10 to 80°C.

HPLC. Triacylglycerols (TAGs) were analyzed by Shukla *et al.* method (20). The HPLC columns consisted of two 150 mm × 4.6 mm i.d. in series. They were packed with 3 μm C18 bonded-phase particles. The columns were maintained at 40°C by a column oven. The analyses were carried out by mixing acetonitrile and tetrahydrofuran (70:30, vol/vol) at 0.6 mL/min, the usual flow rate. The laser light-scattering detector was used to identify the separated TAGs. TAGs were also separated with capillary GC and an HPLC argentated column (21). The column size was 250 mm × 4.6 mm i.d. and was packed with 5 μm Lichrosorb Si 60 argentated silica. Benzene was used as the mobile phase at the flow rate of 0.5 mL/min. A refractive index detector was used.

RESULTS

Effects of preheating. Figure 2 corresponds to T_c 25.4°C, the lowest selected. Even at this temperature, the amount of crystals at the top of the signal was small, and only a few were obtained after filtering. This temperature is high as compared to the MDP 35 of the sample.

Table 1 shows the induction times observed for the two thermal treatments at different T_c values, as well as the

TABLE 1

Induction Times and Cooling Rates at Five Crystallization Temperatures (T_c)

T_c (°C)	Thermal treatment[a]	τ (min)	Cooling rate (°C/min)
30.7	a	101.4 ± 2.1	3.6
	b	83.6 ± 1.8	1.4
28.7	a	51.6 ± 1.9	4.3
	b	30.1 ± 0.6	1.8
27.7	a	34.5 ± 0.8	4.6
	b	25.4 ± 0.9	1.8
26.7	a	23.5 ± 0.9	5.7
	b	13.1 ± 0.4	1.8
25.4	a	14.8 ± 0.6	4.1
	b	9.7 ± 0.2	1.8

[a]Treatments: a, 30 min at 80°C; b, 1 h at 65°C followed by 30 min at 40°C.

calculated cooling rate for each case. Two different effects are present here, preheating treatment and cooling rate. It can be observed (Table 1) that samples, melted at 65°C for 1 h and kept at 40°C for 30 min, showed shorter induction times at all T_c. In addition to that, the induction time for crystallization was markedly dependent on the T_c.

This thermal treatment was also coincident with the slow cooling rate. To separate the two effects, hydrogenated sunflowerseed oil was temperature-cycled, heated at 80 or 65°C and then preheated for 10, 20 and 30 min at 40°C during the first, second and third cycle, respectively. Induction times were 29.7, 30.1 and 29.8 min for 80°C and 29.6, 29.7 and 30.2 for 65°C. No differences were found in induction times. There was no faster crystallization after the second and third cycle.

It is more probable that the differences in Table 1 are an effect of the cooling rate. At fast cooling rate, the α form can be expected, whereas at a slow rate we should get β' or β. The α-form has the shortest induction time and the β-form the longest. At fast cooling rates, induction times were longer, and they were shorter at slow rates. If polymorphism were responsible for differences in induction times, the expected result would be the opposite.

Relationship between cooling rate, morphology and polymorphism. To better understand this behavior, the morphology and crystal habit of the first-occurring crystals were carefully observed. Figure 3 shows the morphology obtained for the two thermal treatments when the sample was cooled down to 27 and 30°C. There were no differences in morphology for the two treatments at these two crystallization temperatures. Spherulitic patterns of the β' form were observed in all cases. The spherulites are well organized and show a needle structure, with the needles clearly run outward radially. At 30°C, there was a smaller amount of crystals than at 27°C. The photograph shows that the needles that form the spherulites were less densely packed at the highest temperature.

When the laser signal reached its peak, crystals were filtered and their polymorphic behavior was studied from XRD long and short spacings. In all cases, crystals were in the β' form. The patterns showed four signals at 3.9, 4.1, 4.3 and 4.4 . In this complex system, only one β' pattern was obtained. It was not possible to distinguish the two forms of β'_1 and β'_2. The long spacings were also similar. Signals at 15.2 and 40.2 were found in all cases. They correspond to a double chainlength arrangement. These signals disappeared when samples were melted. No change was found when the temperature was raised.

As mentioned before, the amount of crystals was small when the laser signal reached its peak. To study thermal behavior, chemical composition and polymorphic transformation rate, crystals were kept growing at night and then were filtered.

Figure 4 shows the DSC diagrams obtained for the two thermal treatments at 27 and 30°C. Thermal behavior changed with cooling rate at both T_c values. At 27°C, two endotherms were found at the slow rate (Fig. 4a). The second one was broad with three peaks which were not

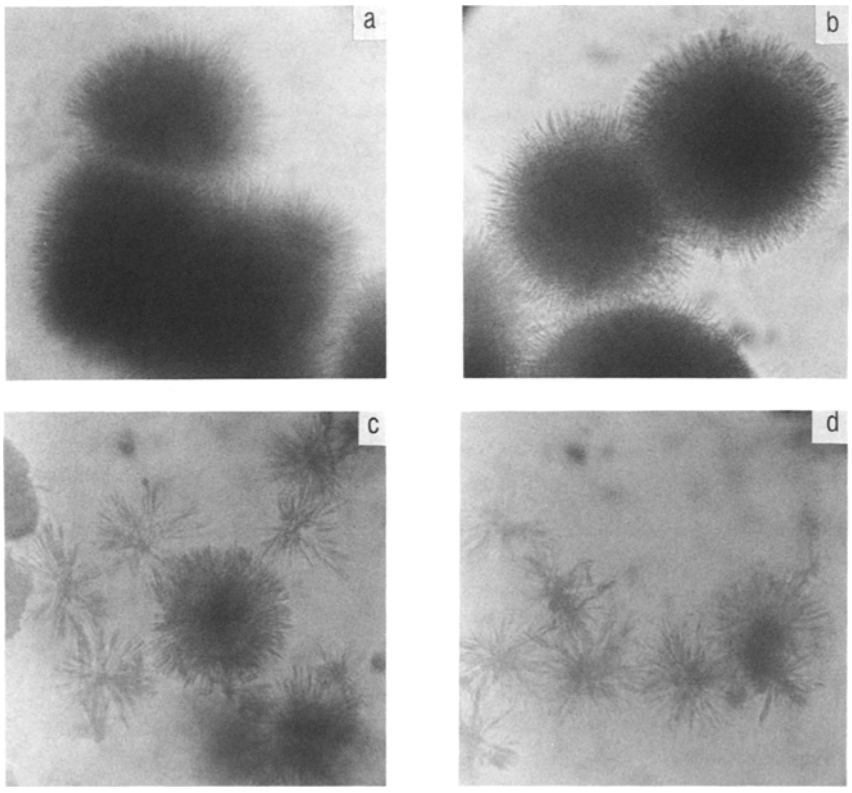

FIG. 3. Morphology of the crystals. Crystallization temperature T_c = 27°C; a, preheated 1 h at 65°C followed by 30 min at 40°C; b, preheated 30 min at 80°C. T_c = 30°C; c, preheated 1 h at 65°C followed by 30 min at 40°C; d, preheated 30 min at 80°C.

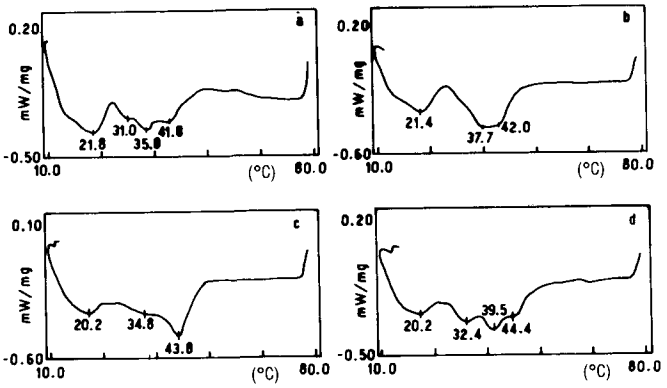

FIG. 4. Differential scanning calorimetry melting thermograms of the crystals corresponding to the photographs of Figure 3.

completely resolved. Their peak temperatures were 31.0, 35.8 and 41.8°C. Even after a night of growing at 27°C, the XRD diagram showed a β' pattern. At the fast rate, two endotherms were also found (Fig. 4b). The second one was formed by two peaks of 37.7 and 42.0°C, and they were too close to be resolved. After a night growing, the XRD pattern also corresponded to the β' form. Because of its high content of elaidic acid in the different positions of the glycerol group, hydrogenated sunflowerseed oil may have a special polymorphic behavior. The β' form is stable and, even at high crystallization temperatures, it is the form generally obtained at both fast and slow rates. However, diagrams of the DSC profiles were different. For all crystallization temperatures, except for 30°C, the same thermal behavior was found. At the slow rate, fractionation occurred and a second broad endotherm with more peaks appeared that were not completely resolved. Differences in the diagrams of the DSC profile were probably not due to the polymorphic transition of β' to β because, for both fast and slow rates, a melting rate of 5°C/min was used to obtain the thermograms. A slow cooling rate seems to make for easier crystallization if the fact that induction times are shorter at all crystallization temperatures is taken into account.

At $T_C = 30$°C, and slow rate, a β pattern was found after 24 h as well as a DSC diagram with a well-defined second peak at 43.8°C and a shoulder at 34.8°C (Fig. 4c). On the other hand, after a night of growing, crystals were a mixture of β' and β when the sample were preheated 30 min at 80°C (Fig. 4d). In this case, at fast rate, a broad second endotherm with peak temperatures of 32.4, 39.5 and 44.4°C was found by DSC. The diagrams' profiles show that the shape at fast rate, when the sample was crystallized down to 30°C, is similar to that found at slow rate for the other crystallization temperatures. At 30°C, a mixture of β' and β forms was found. In all other cases, only the β' form was found. The broad second endotherm obtained at fast rate at $T_C = 30$°C is the result of the melting of different polymorphic forms.

Chemical composition of the crystals. Octadecylsilyl HPLC (ODS-HPLC), argentated silica HPLC ($AgNO_3$-HPLC) and capillary GC were used to determine the chemical composition of the crystals (Table 2). *Trans* acid content was high and similar for the two crystallization temperatures. No differences were found between the two

TABLE 2

***Trans* Fatty Acid and Triacylglycerol Composition of the Crystals Obtained When Sample was Crystallized at 27 and 30°C[a]**

Sample	*trans* Acids[b] (%)	ODS-HPLC ECN (%) 46	48	50	52	GC capillary CN (%) 50	52	54
T_c27°C b	48.3	12.4	57.7	27.0	1.6	2.1	23.9	74.0
a	48.5	11.6	56.3	28.2	2.0	3.1	25.3	71.6
T_c30°C b	47.3	13.6	58.1	25.2	1.5	2.5	25.9	71.5
a	48.4	12.8	57.5	27.6	1.9	1.8	23.7	74.5

[a]ODS-HPLC, octadecylsilyl high-performance liquid chromatography; ECN, equivalent carbon number; CN, carbon number; T_c, crystallization temperature.
[b]Treatments a and b as in Table 1.

thermal treatments. Elaidic acid is the principal *trans* isomer in these samples. Only about 1-2% are other fatty acids. Triacylglycerol analysis by ODS-HPLC showed four principal equivalent carbon numbers (ECN): 46, 48, 50 and 52. The most probable triacylglycerols were the following: for ECN 46, LOO (L, linolenic acid; O means *cis* + *trans* isomers); for ECN 48, POO and OOO for ECN 50, SOO; and for ECN 52, SSO. The percentages were similar for all samples.

To improve the information of ODS-HPLC analysis, $AgNO_3$-HPLC and capillary GC were performed. From the $AgNO_3$ analysis, the number of double bonds of the triacylglycerols was determined. The triacylglycerols that exhibited higher percentages were SOS, SOO, POO, OOO and LOO. Capillary GC generated three peaks that contained more than one triacylglycerol. C50 corresponds to POP and PLP; C52 to POS, POO, PLS, PLO and PLL, and C54 to SOS, SOO, OOO, OLO, LLO and LLL. The percentages were similar for all samples.

From these results, we conclude that differences found in thermal behavior and induction times are not due to differences in chemical compositions. Instead, interactions between the triacylglycerols must be responsible.

Polymorphic transformation rate. Figure 5 shows XRD diagrams of the samples crystallized at 27 and 30°C at different storage times. When a sample was crystallized at 27°C and preheated for 30 min at 40°C (Fig. 5a), after a night of growing the XRD pattern corresponded to the β' form. Four lines at 4.4, 4.3, 4.1 and 3.9 appeared. After 48 h at 25°C, a signal at 4.6 was found, which means the existence of a mixture of β' and β forms. After nine days at 25°C, the pattern corresponded to the β form. Nine days were enough to complete the polymorphic transformation. When preheated 30 min at 80°C (Fig. 5b) a β' diagram was also obtained after a night of growing. The polymorphic transformation from β' to β started after 48 h, but after nine days, a mixture of β' and β forms still remained. Complete transformation occurred after 35 d. At 30°C, when the sample was kept 30 min at 40°C (Fig. 5c), a β pattern was obtained after a night of growing. A weak signal at 4.3 also appeared but disappeared after two days. When the sample was preheated 30 min at 80°C (Fig. 5d), a mixture of β' and β crystals was found. Four strong signals at 4.6, 4.4, 4.3 and 3.9 and two weak ones at 4.1 and 3.8 appeared. After a week at 25°C, polymorphic transformation was complete. In both cases, the rate of polymorphic transformation was slower when induction

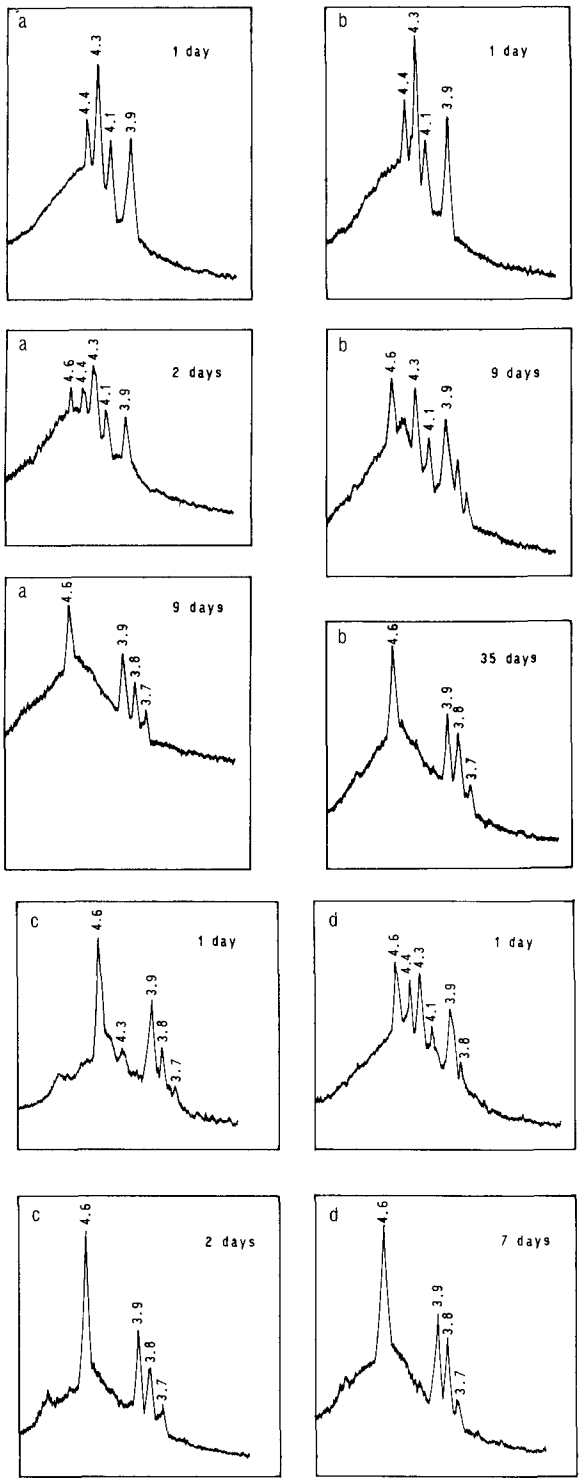

FIG. 5. X-ray diffractometry patterns of the crystals corresponding to the photographs of Figure 3.

times were longer. Polymorphic transformation was easier for shorter induction times.

Changes in crystal morphology during transformation. When a sample was kept for 1 h at 65°C, followed by 30 min at 40°C and then crystallized at 30°C, the first-occurring crystals were in the β' form, and their morphology is shown in Figure 3. After 6 h at 30°C, the morphology was as shown in Figure 6a. β' Spherulites were still observed, together with β crystals. After 48 h at 30°C (Fig. 6b), the XRD diagram of crystals corresponded to the β form. The crystals were spherulitic, but seemed less organized in their packing.

It is difficult to identify polymorphism on the basis of microscopic appearance. β' and β crystals do not look much different, even if XRD patterns clearly correspond to one of the polymorphic forms, β' or β.

DISCUSSION

It is known that mixtures of triacylglycerols similar in melting points form solid solutions over extensive, but not usually complete, ranges of composition. This leads to several types of phase behavior, eutectic formation being the most common, although peritectics and monotectics are also formed (22).

The chemical composition points to the way in which triacylglycerols containing elaidic acid behave and gives to this hydrogenated oil a special crystallization behavior. Semi-solid natural fats, such as palm oil, which does not contain *trans* isomers, crystallized in the β' or β form, depending on the crystallization temperature. Polymorphic studies showed that thermal properties and structural behavior of elaidic- and stearic-containing triacylglycerols are different from oleic-containing triacylglycerols (13). PEE behaves like PPP and EEE. *Trans* unsaturation in a triacylglycerol influences β' stability. The

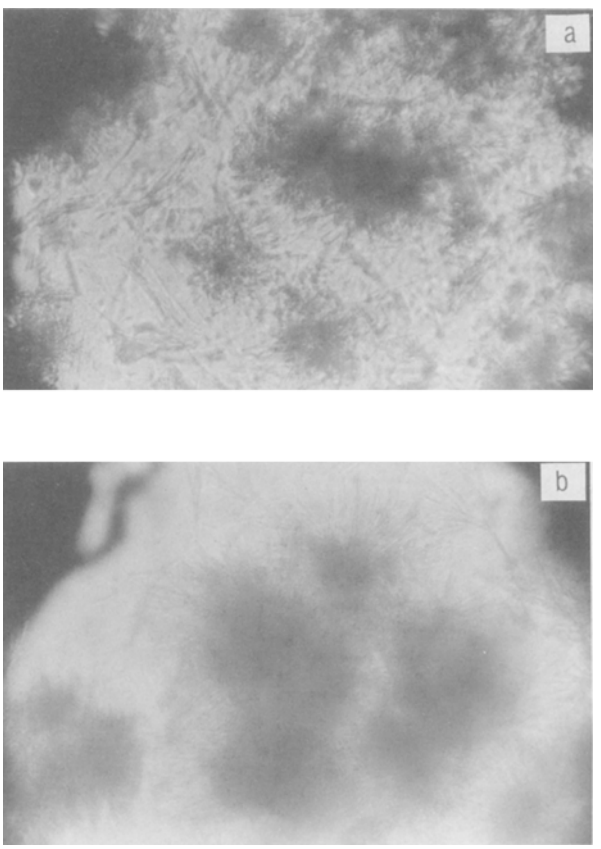

FIG. 6. Morphology of the crystals. T_c = 30°C; a, after 6 h; b, after 48 h. Abbreviations in Figure 3.

β' form was not observed in EEE. However, when triglycerides with elaidic and palmitic chains all together crystallize from solvents, transformation into the β form is slow. In this case the β form was not found in PEE. The most stable form was pseudo β'_{1-2} . The oleic–palmitic triglycerides OPP and POO showed the same behavior (13).

When triacylglycerols crystallize from a complex mixture, they interact to each other. Because triacylglycerols with elaidic and oleic chains have different melting behavior, the PPP/EEE system makes an interesting comparison with the PPP/OOO system. The thaw point for OOO-rich mixtures would be roughly 4°C, but for the corresponding EEE-rich mixtures it is about 40°C. The EEE/OOO system has also been studied by the thaw-melt method. This liquid's curve is similar in shape to that of the SSS/OOO system. Information obtained for the solids line showed a low (less than 10%) solubility of OOO in solid EEE, in contrast with other systems involving elaidyl glycerols, where solid solutions are often formed over extensive composition ranges (22).

Hydrogenated sunflowerseed oil shows a stable β' form when it crystallizes. In this complex mixture, palmitic–elaidic triacylglycerols behave like the pure triacylglycerols when they crystallize from solvents. Cooling rate seems to affect the interactions between triacylglycerols. At slow rate, fractionation occurred as expected. In the hydrogenated sunflower oil, 48% of C18:1 was elaidic acid and 52% was oleic acid. Elaidic and oleic triacylglycerols were not expected to form solid solutions in these concentrations.

Sunflowerseed oil crystallizes in the β' form under a wide range of cooling rates. Neither α nor β crystallization was found. The β' form is stable and transforms to β in different times, depending on the storage temperature and cooling rate selected.

ACKNOWLEDGMENTS

A grant supporting this work was obtained from Consejo Nacional de Investigaciones Cientificas y Tcnicas (CONICET), República Argentina. Thanks to Hiroshima University for providing all the equipment used in this study.

REFERENCES

1 Hvolby, A., *J. Am. Oil Chem. Soc. 51*:50 (1974).
2. Rivarola, G., J.A. Segura, M.C. Añón and A. Calvelo, *Ibid. 64*:1537 (1987).
3. Sahasrabudhe, M.R., and C.J. Kurian, *J. Inst. Can. Sci. Technol. 12*:140 (1979).
4. Carpenter, D.L., J. Lehmann, B.S. Mason and H.T. Slover, *J. Am. Oil Chem. Soc. 53*:713 (1976).
5. Nazis, D.J., B.J. Moorecroft and M.A. Mishkel, *Am. J. Clin. Nutr. 29*:331 (1976).
6. Chow, Ch.K., *Fatty Acids in Foods and Their Health Implications*, edited by Ch.K. Chow, Marcel Dekker, Inc., New York, 1992, p. 25.
7. Lo, L.C., and A.P. Handel, *J. Am. Oil Chem. Soc. 60*:815 (1983).
8. Timms, R.F., *Prog. Lipid Res. 23*:1 (1984).
9. deMan, L., V. D'Souza, J.M. deMan and B. Blackman, *J. Am. Oil Chem. Soc. 69*:246 (1992).
10. Small, D.M., *The Physical Chemistry of Lipids*, edited by Donald J. Hanahan, Plenum Press, New York, 1986, p. 377.
11. Perron, R., J. Petit and A. Mathieu, *Chem. Phys. Lipids 3*:1 (1969).
12. Gibon, V., P. Blanpain, F. Durant and C. Deroanne, *Belgian J. of Food Chem. and Biotechnol. 40*:119 (1985).
13. Desmedt, A., Etude des propriétés structurales et thermiques de triglycérides purs et en présence d'émulsifiants. Influence de la nature de la chaîne en C18 et application au phénomène de blanchiment, Ph.D. Thesis, Facultes Universitaires, Notre-Dame de la Paix, Namur, 1993.
14. Herrera, M.L., J.A. Segura and M.C. Añón, *J. Am. Oil Chem. Soc. 68*:793 (1991).
15. Herrera, M.L. and M.C. Añón, *Ibid. 68*:799 (1991).
16. Herrera, M.L., J.A. Segura, G.J. Rivarola and M.C. Añón, *Ibid. 69*:898 (1992).
17. Chong, Ch.L., and K. Sato, *INFORM 4*:537 (1993).
18. Herrera, M.L., and K. Sato, *Ibid. 5*:553 (1994).
19. Marc Kellens, Polymorphism of Saturated Monoacid Triglycerides, Ph.D. Thesis, Catholic University of Leuven, Notre-Dame de la Paix, Leuven, 1991.
20. Shukla, V.K.S., W.S. Nielsen and W. Batsberg, *Fette. Seifen. Anstrichm. 85*:274 (1983).
21. Smith, E.C., A.D. Jones and E.W. Hammond, *J. Chomatogr. 188*:205 (1980).
22. Rossell, J.B., *Advances in Lipid Researches 5*:353 (1967).

[Received April 3, 1994; accepted July 6, 1994]